

## ON/OFF SWITCHABLE HIGH- $Q$ CAPACITIVE-PIEZOELECTRIC ALN RESONATORS

*Robert A. Schneider and Clark T.-C. Nguyen*

Berkeley Sensor & Actuator Center, University of California, Berkeley, CA, USA

### ABSTRACT

Voltage-controlled on/off switching based on electrode collapse around a 301-MHz capacitive-piezoelectric AlN contour-mode disk resonator has been demonstrated while still allowing on-state  $Q$ 's as high as 8,800—the highest yet demonstrated around 300MHz in sputtered AlN. The key to on/off switching of this device is the structure of its capacitive-piezoelectric transducer, which provides a suspended electrode atop the suspended AlN resonator that can be pulled electrostatically towards the substrate, pinning the combined resonator-electrode structure to the substrate, thereby opening new conduits for energy loss that suppress signal transmission. This on/off switchability obviates the signal path micromechanical switches needed by conventional attached-electrode AlN resonator counterparts. The  $Q$  approaching 9,000, together with the demonstrated on/off switchability and electromechanical coupling  $k_{eff}^2$  up to 0.78%, make this capacitive-piezoelectric resonator a strong contender among resonator technologies targeting RF channel-selecting communication front-ends.

### INTRODUCTION

RF channel-selection promises to reduce noise and suppress interferers in wireless transceivers [1], yet research efforts confront a daunting challenge: the need for a switchable bank of small percent bandwidth filters. So far, neither piezoelectric nor capacitively transduced resonators can provide the simultaneous high- $Q$ , high electromechanical coupling ( $k_{eff}^2$ ), low motional resistance ( $R_x$ ), self-switchability, and power handling needed to select individual channels over a wide RF range. Indeed, each technology provides only a subset of the desired properties.

Channel-selecting filters require higher  $Q$ 's than the 2,100's conventional AlN resonators can currently deliver [2]. To illustrate, Figure 1 presents low- $Q$  and high- $Q$  simulations for 0.25% bandwidth 2<sup>nd</sup>, 3<sup>rd</sup>, and 4<sup>th</sup> order filters, for which insertion loss improves dramatically with  $Q$ 's of 8,800. Since insertion loss (which equates to noise figure), increases as bandwidth drops, the minimum achievable bandwidth is inversely dependent on the  $Q$ 's of a filter's constituent resonators. High- $Q$  is thus essential: it allows for higher-order filters, reduced noise, and freedom to reduce a filter's bandwidth.

Capacitive gap transduced resonators are of great interest because they achieve very high  $Q$ 's at UHF frequencies, e.g.,  $Q$ 's over 40,000 at 3GHz, that satisfy the needs of RF channel-selection [3]. They are also self-switchable via a DC bias—helpful for implementing filter banks without the signal path switches of Figure 2(a), which add 0.2-0.5dB of insertion loss and require substantial on-chip real estate [4], so increase cost. Self-switching filters, shown in the architecture

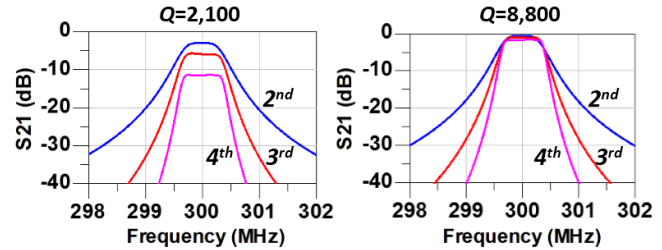


Figure 1: Simulated 0.25%-bandwidth 2<sup>nd</sup>, 3<sup>rd</sup>, and 4<sup>th</sup> order Chebyshev micromechanical filter responses using low- $Q$  and high- $Q$  constituent resonators.

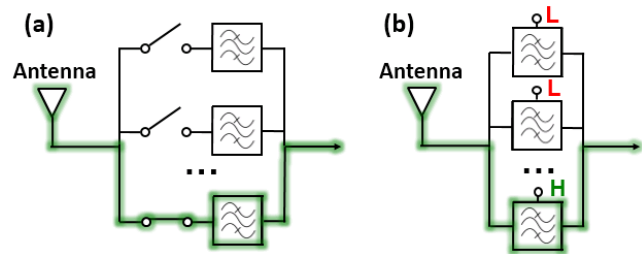


Figure 2: (a) Filter bank architecture requiring series switches. (b) Improved design with self-switched devices.

of Figure 2(b), are preferable, as they dispense with the need for such switches. Unfortunately, capacitive resonators are often plagued by very high  $R_x$  and insufficient  $k_{eff}^2$ , precluding their use in many applications.

On the other hand, piezoelectric contour-mode AlN resonators offer very low  $R_x$ , high  $k_{eff}^2$ , and strong power handling, excelling where capacitive resonators struggle. However, in addition to their much lower  $Q$ 's, traditional AlN resonators currently lack a self-switching capability, meaning they can only be used to implement the undesirable filter bank architecture of Figure 1(a). Pursuant to solving these problems, this paper introduces methods for improving the  $Q$ 's of piezoelectric AlN contour-mode resonators while simultaneously making them self-switchable.

### SWITCHABLE RESONATOR DESIGN

Figure 3(a) presents a perspective-view schematic of the demonstrated on/off switchable capacitive-piezoelectric AlN resonator. Like the device of [5], separating the electrodes from the resonant structure and suspending them at close distance eliminates energy loss from lossy metal electrodes and from the metal-to-piezoelectric interface. The resultant increase in  $Q$  does come at the cost of marginally reduced  $k_{eff}^2$  due to reduction in electric field strength in the AlN when electrode-to-resonator gaps are introduced. Design parameters for the 300-MHz resonator, including the frequency-set-

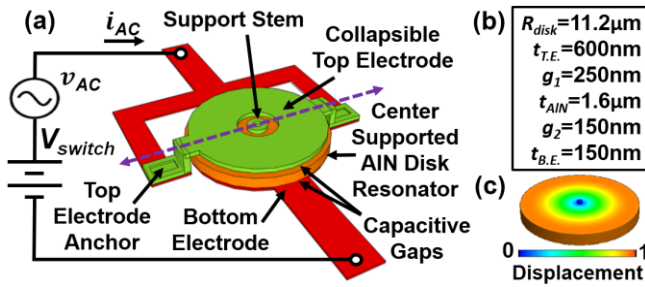


Figure 3: (a) Perspective-view schematic of the 300-MHz switchable capacitive piezoelectric disk resonator of this work. (b) Device dimensions. (c) FEM-simulated radial-contour mode shape at 300 MHz.

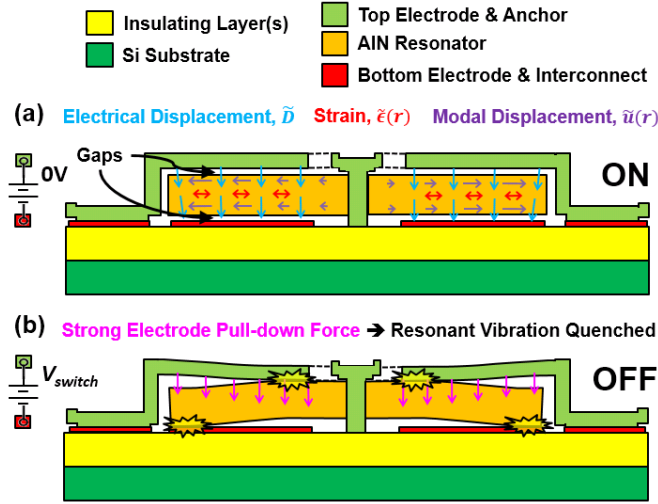


Figure 4: Disk resonator cross-sections corresponding to the vertical plane of the purple dashed line in Figure 3. (a) ON State:  $V_{switch}=0V$  and the device resonates freely. (b) OFF State:  $V_{switch}$  incites pull-down of the top plate and collapse of the structure to impede resonance.

ting disk radius and vertical layer dimensions in top-down order, are given in Figure 3(b). Figure 3(c) presents the radial-contour modal displacement field at the predicted eigenfrequency.

The key to on/off switching of this device is the structure of its capacitive-piezoelectric transducer, which provides a suspended electrode atop the suspended AIN resonator that can be pulled electrostatically towards the substrate, pinning the combined resonator-electrode structure to the substrate, thereby opening new conduits for energy loss that compromise signal transmission. Figure 4 presents cross sections of the switchable disk for both the ON and OFF states. In the ON state, *cf.* Figure 4(a), an input voltage  $v_{AC}$  between the top and bottom electrodes drives the device into resonant vibration through the reverse piezoelectric effect, in the absence of a DC switching voltage.

To shut the device OFF, one merely applies a switching bias voltage  $V_{switch}$  between the top and bottom electrodes until the electrostatic force acting downward on the top electrode is large enough to pull the top plate down, taking with it the AIN resonator structure so that both end up pinned to

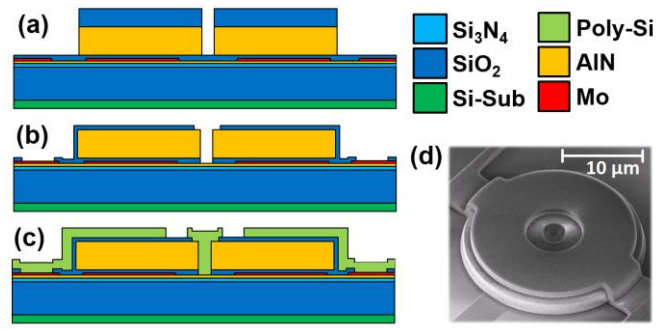


Figure 5: Fabrication process illustration. (a) Post AIN etch. (b) Post anchor etch. (c) Post polySi etch, pre-release. (d) SEM of the completed device.

the substrate. With top and bottom electrodes abutted against, but not attached, to the AIN structure, frictional loss becomes quite large. In addition, direct contact of the resonator with the substrate, without the Bragg reflectors used by solidly-mounted resonators (SMR's) [6], also steals considerable energy. All told, the energy loss inflicted by voltage-induced collapse is large enough to completely remove the resonant peak. Of course, the real magic of such a device is the ability to turn ON again. Upon removal of the switching voltage, the top plate springs back up, resuming normal operation.

## DEVICE FABRICATION

The fabrication process of this work includes four lithography steps and allows for versatile top electrode configurations through the use of a conformal CVD doped polysilicon deposition. The process begins with a 150mm wafer upon which 2 $\mu\text{m}$  of  $\text{SiO}_2$  is grown, for electrical isolation, followed by a 250nm low-stress silicon nitride deposition to protect the underlying oxide during a future release step. Since the release will be done via vapor HF, a 100-nm-thick AIN layer is sputter deposited above the silicon nitride to act as a barrier layer to mitigate silicon nitride's incompatibility with vapor HF etching. In retrospect, this AIN layer should be kept as thin as possible, or eliminated altogether, to minimize piezoelectric coupling to the substrate.

150nm of molybdenum is then sputter deposited and dry-etched in an  $\text{SF}_6$  plasma to form the bottom interconnect layer. Next, 300nm of low temperature oxide (LTO) is deposited, followed by a quick CMP ( $\sim 150\text{nm}$ ) to eliminate surface topography whilst forming a thin sacrificial layer. 1.6 $\mu\text{m}$  of AIN is then sputter deposited in a Tegal Endeavor AT system to form the resonator, followed by LPCVD deposition of a 1- $\mu\text{m}$ -thick LTO oxide to serve as a hard mask during AIN etching. After patterning the hard mask to delineate resonator features and expose AIN, the AIN is dry etched using a 90/35/10 sccm  $\text{Cl}_2/\text{BCl}_3/\text{Ar}$  etch chemistry, resulting in the cross section depicted in Figure 5(a), followed by a final oxide etch to remove the hard mask above the resonators. A final 250-nm-thick LTO deposition then follows to define the top sacrificial electrode-to-resonator gap spacer, which is patterned in the third lithography step to define anchor openings to the substrate, *cf.* Figure 5(b).

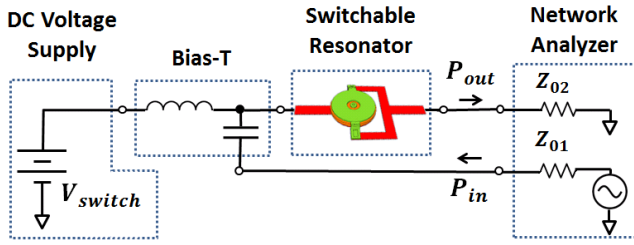


Figure 6: Experimental setup to measure impedance and apply a DC switching voltage to a switchable resonator.

Finally, a dual purpose 600-nm-thick LPCVD doped polysilicon deposition forms the supporting stem for the disk as well as the top collapsible electrode. After a final lithography step and plasma etch to pattern the polysilicon electrode, *cf.* Figure 5(c), the wafer is cleaved. Devices are cleaned and put on a hot plate at 200°C prior to release in a Primaxx vapor HF etch system. Figure 5(d) presents the SEM of a completed device.

## EXPERIMENTAL RESULTS

Figure 6 presents a schematic of the test setup used, where a DC switching voltage  $V_{switch}$  is added to the input RF signal using a bias-T. On-state operation of the switchable resonator entails applying an AC input voltage and sensing the output current while the DC switch-control voltage  $V_{switch}$  is turned off. At 300 MHz, this is best implemented using the microwave test setup shown, where the passive switchable resonator, held under vacuum for maximum  $Q$ , has a highly frequency-selective impedance to be characterized. Here, a two-port S-parameter measurement is performed, despite being a one-port device, because the parameter of greatest interest for a filter is its signal transmission. Although a single resonator is measured in this experiment, the same measurement method can be used for a higher-order filter of multiple coupled resonators. Also, since the impedance of a single device is on the order of 1-10 k $\Omega$ , a two-port measurement provides a more accurate estimate of impedance than does a one-port measurement, for which a small calibration error results in a large error in measured admittance. The resonator parameters  $R_x$ ,  $Q$ , and  $k_{eff}^2$  for a device are extracted directly from the  $S_{21}$  frequency characteristic measured by the network analyzer as follows:

$$R_x = 2Z_0(-1 + 10^{-S_{21,dB}/20}) \quad (1)$$

$$Q = (f_{peak}/\Delta f_{3dB})(R_x + 2Z_0)/R_x \quad (2)$$

$$k_{eff}^2 = (\pi^2/4)(f_p - f_s)/f_s \quad (3)$$

where  $Z_0 = Z_{01} = Z_{02} = 50\Omega$  represent the characteristic impedances of the measurement system,  $f_s = f_{peak}$  is the series resonance frequency at which maximum transmission occurs,  $\Delta f_{3dB}$  is the 3-dB bandwidth around the  $f_s$  peak, and  $f_p$  is the parallel resonance frequency.

### On/Off Switchability

To characterize the on/off switchability of the device,  $S_{21}$  measurements are made in between repeated transitions between the ON and OFF states of  $V_{switch}=0V$  and  $V_{switch}=220V$ ,

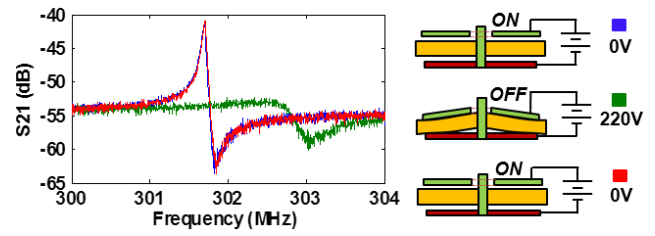
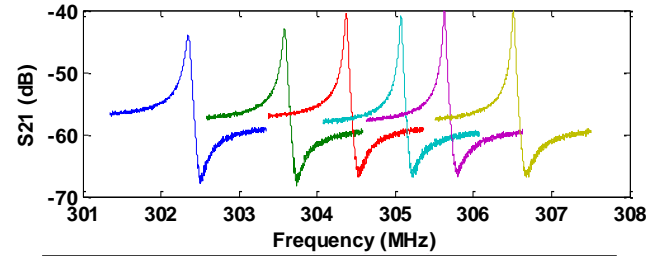


Figure 7: Demonstration of switching capability. The resonator is ON when no switching voltage is applied. Next, a DC voltage of 220V is applied, causing the top electrode to collapse, effectively turning the device OFF. When the switching bias is removed, the resonator turns back ON, with no degradation in performance.



S. D.	2.2 $\mu\text{m}$	2.0 $\mu\text{m}$	1.8 $\mu\text{m}$	1.6 $\mu\text{m}$	1.4 $\mu\text{m}$	1.2 $\mu\text{m}$
Color	<span style="color:blue">●</span>	<span style="color:green">●</span>	<span style="color:red">●</span>	<span style="color:cyan">●</span>	<span style="color:magenta">●</span>	<span style="color:yellow">●</span>
$Q$	4,743	5,924	7,609	8,416	8,431	8,757

Figure 8:  $Q$  and resonance frequency dependence on stem diameter for six adjacent resonators.

respectively. Figure 7 presents three superposed  $S_{21}$  measurements made before, while, and after applying the needed switching voltage, as well as device cross sections. The measurements made before and after turning the device off are virtually identical and the measurement was cycled 20 times with no failure or initial frequency or  $Q$  changes over the duration of the experiment.

Here, the needed pull-down voltage of 220V is high, but not dissimilar from voltages normally needed to actuate RF MEMS switches. The good news is smaller gaps and proper device suspension design can make the needed voltages much smaller. Numerous approaches toward achieving this goal warrant further investigation, including single point electrode anchoring and folded beam electrode suspensions, as are used for some MEM relays, as well as their fabrication techniques [7].

### High- $Q$ Operation

While capacitive piezoelectric transduction is essential to maximizing  $Q$ , anchor minimization and post-release cleaning are equally important. Figure 8, which plots  $S_{21}$  as a function of stem diameter, shows how the  $Q$ 's of these devices also depend strongly on the widths of their stem anchors. Here, the smallest anchor diameter of 1.2  $\mu\text{m}$  yields a measured  $Q$  of 8,757, which is almost twice that of a 2.2  $\mu\text{m}$ -stem version, and 4.2 $\times$  higher than the  $\sim 2,100$  typically reported for conventional AlN resonators in this frequency range [2]. The resonance frequency changes seen in Figure 8

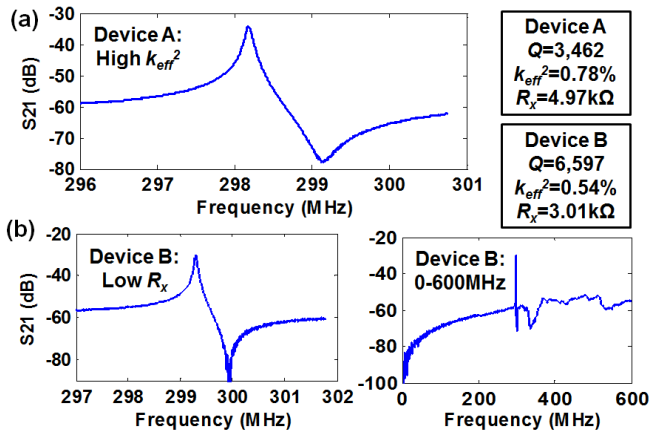


Figure 9: (a) Frequency response for Device A with a high measured  $k_{eff}^2$  of 0.78%. (b) Frequency response for Device B with a  $k_{eff}^2$ - $Q$  product of 35.6 and an  $R_x$  of 3.01k $\Omega$ . The wideband response for Device B shows no spurious mechanical modes from DC to 600 MHz.

agree with predictions that estimate resonance frequency as a function of polysilicon anchor size.

After release, the devices have poor  $Q$ 's of only several hundred. One probable reason revealed upon SEM inspection is that a thin layer of etch residue remains on the surface of the disks right after release. A post-release procedure comprised of dipping the devices in DI water for several minutes, drying with an  $N_2$  gun, and placing on a hotplate at 200°C in air for several minutes, reliably raises  $Q$ 's up to 6,000. A 5 minute anneal at 500°C in an  $N_2$  environment yields further  $Q$ -improvement, as was done in [5], and was necessary to achieve  $Q$ -values above 8,000.

### Strong Electromechanical Coupling

Pursuant to increasing the  $k_{eff}^2$ 's and lowering the  $R_x$ 's of these resonators, the process was rerun on a second wafer with more aggressive gap spacings of 120-150 nm. Through a combination of smaller gaps and better AlN quality, a 4 $\times$  reduction in  $R_x$  (for devices of comparable  $Q$ 's) and a 2 $\times$  increase in  $k_{eff}^2$  were realized. However, due to a problem at the anchor etch step arising from changing to a 1.5 $\mu$ m-thick polySi interconnect, only a small subset of devices survived the release that unfortunately did not include the devices with very small anchors for maximum  $Q$ . Stem diameters are 1.8 $\mu$ m for the measured disks.

As expected, the  $k_{eff}^2$ 's on the order of the 0.78% measured in Figure 9(a) are smaller for these capacitive-piezoelectric resonators than for conventional contour-mode AlN resonator counterparts (with attached electrodes), but they are nonetheless much larger than achieved by capacitive-gap transduced devices at this frequency, and more importantly, are plenty large enough to satisfy the needs of channel-selecting RF front-ends.

Strong evidence of the efficacy of capacitive piezoelectric transduction is presented in Figure 9(b), which demos a  $k_{eff}^2$ - $Q$  product of 35.6 on par with the 31.5 and 39.9 exhibited by the conventional attached electrode counterparts of [2] at the same frequency. Additionally, Figure 9(c) presents a

clean, spur-free wideband response for the same resonator over a 600MHz range, indicating the device's superior ability to excite a single desired mode shape.

Looking forward, based on measurements of devices on each of the two runs,  $k_{eff}^2$ - $Q$ 's on the order of 70 are not unreasonable to expect for this device, as are single disk motional impedances of 1-2k $\Omega$ . If achievable, such individual disks, when mechanically combined to form array resonators, could realize sub-100 $\Omega$   $R_x$ 's, making them amenable to low impedance termination in practical RF systems.

## CONCLUSIONS

With this work, capacitive-piezoelectric resonators have demonstrated not only  $Q$ 's approaching 9,000 at 300MHz, but also a new on/off switching capability, both of which represent important first steps toward implementing switchable AlN channelizing filter banks for RF front ends. Although more extensive study is needed on the reliability of the collapse-based switching mechanism, this technology certainly raises eyebrows and encourages work towards developing higher-order filters that harness the high  $Q$  and self-switching. Such work is ongoing.

## ACKNOWLEDGEMENTS

The authors would like to thank the staff of the Berkeley Nanolab and Zeying Ren for valuable assistance. This work was supported by the DARPA CSSA program.

## CONTACT

\*Robert Schneider, [schneid@berkeley.edu](mailto:schneid@berkeley.edu)

## REFERENCES

- [1] C. T.-C. Nguyen, "Integrated micromechanical circuits for RF front ends," in *Solid-State Device Research Conference, 2006. ESSDERC 2006. Proceeding of the 36th European*, 2006, pp. 7–16.
- [2] C. Zuo, N. Sinha, and G. Piazza, "Very high frequency channel-select MEMS filters based on self-coupled piezoelectric AlN contour-mode resonators," *Sens. Actuators Phys.*, vol. 160, no. 1, pp. 132–140, 2010.
- [3] T. L. Naing, T. Beyazoglu, L. Wu, M. Akgul, Z. Ren, T. O. Rocheleau, and C. T.-C. Nguyen, "2.97-GHz CVD diamond ring resonator with  $Q > 40,000$ ," in *Frequency Control Symposium (FCS), 2012 IEEE International*, 2012, pp. 1–6.
- [4] S. S. Li, Y. W. Lin, Z. Ren, and C. T.-C. Nguyen, "Self-switching vibrating micromechanical filter bank," in *Frequency Control Symposium and Exposition, 2005. Proceedings of the 2005 IEEE International*, pp. 135–141.
- [5] L. W. Hung and C. T.-C. Nguyen, "Capacitive-piezoelectric AlN resonators with  $Q > 12,000$ ," in *Micro Electro Mechanical Systems (MEMS), 2011 IEEE 24th International Conference on*, 2011, pp. 173–176.
- [6] K. M. Lakin, K. T. McCarron, and R. E. Rose, "Solidly mounted resonators and filters," in *Ultrasonics Symposium, 1995. Proceedings., 1995 IEEE*, 1995, vol. 2, pp. 905–908.
- [7] T.-J. K. Liu, L. Hutin, I.-R. Chen, R. Nathanael, Y. Chen, M. Spencer, and E. Alon, "Recent progress and challenges for relay logic switch technology," in *VLSI Technology (VLSIT), 2012 Symposium on*, 2012, pp. 43–44.